RSC Advances

PAPER

View Article Online
View Journal | View Issue

Cite this: *RSC Adv.*, 2024, **14**, 6548

Effects of oregano essential oil Pickering emulsion and ZnO nanoparticles on the properties and antibacterial activity of konjac glucomannan/carboxymethyl chitosan nanocomposite films

Zhibin Pan,†[a] Weiquan Zhong,†[b] Jingting Xu,[b] Danjie Li,[b] Junhan Lin,[a] Weibin Wu,[a] Jie Pang*[b] and Chunhua Wu †*[b]

Green and environmentally friendly natural bio-based food packaging films are increasingly favored by consumers. This study incorporated carboxylated-cellulose nanocrystal stabilized oregano essential oil (OEO) Pickering emulsion and ZnO nanoparticles (ZNPs) into konjac glucomannan (KGM)/carboxymethyl chitosan (CMCS) complexes to develop active food packaging films. The effects of OEO Pickering emulsion and ZNPs on the physical, structural, and antimicrobial activities of the nanocomposite films were evaluated. The OEO Pickering emulsion had a droplet size of 48.43 ± 3.56 μm and showed excellent dispersion and stability. Fourier transform infrared and X-ray diffraction analyses suggested that the interactions between the Pickering emulsion, ZNPs and KGM/CMCS matrix were mainly through hydrogen bonding. SEM observations confirmed that the Pickering emulsion and ZNPs were well incorporated into the KGM/CMCS matrix, forming tiny pores within the nanocomposite films. The incorporation of the OEO Pickering emulsion and/or ZNPs obviously increased the light and water vapor barrier ability, thermal stability, mechanical strength and antimicrobial properties of the KGM/CMCS nanocomposite film. Notably, KGM/CMCS/ZNPs/OEO Pickering emulsion films exhibited the highest barrier, and mechanical and antimicrobial activities due to the synergistic effect between the OEO Pickering emulsion and ZNPs. These results suggest that KGM/CMCS/ZNPs/OEO Pickering emulsion films can be utilized as novel active food packaging materials to extend the shelf life of packaged foods.

Received 16th November 2023
Accepted 2nd February 2024

DOI: 10.1039/d3ra07845k

rsc.li/rsc-advances

1. Introduction

The usage of petroleum-based food packaging has led to environmental pollution and concerns regarding food safety. With increased environmental awareness and food safety requirements, many countries and regions are encouraging the production and use of packing films manufactured from naturally derived polymers such as polysaccharides, proteins and lipid.[1] Konjac glucomannan (KGM) and carboxymethyl chitosan (CMCS) are attracting attention as natural biopolymers due to their exceptional properties. KGM is a natural polymer polysaccharide derived from the tubers of the *Amorphophallus Konjac* plant. Its versatility in food packaging applications stems from its exceptional properties, including non-toxicity, biocompatibility, biodegradability, and its ability to form excellent films.[2] CMCS is an amphoteric derivative of chitosan prepared by substituting carboxymethyl into the amino and hydroxyl sites of chitosan.[3] Compared to chitosan, CMCS exhibits superior water solubility and shares the same benefits of non-toxicity, biodegradability, biocompatibility, and excellent film-forming properties. These qualities make CMCS an attractive choice for food packaging applications.[4,5] However, the inherent limitations of pure KGM and CMCS films impede their application in food packaging. KGM films suffer from weak mechanical properties, poor hydrophobicity, and inadequate antimicrobial properties.[6] CMCS films exhibit insufficient antioxidant activity and mechanical strength. A previous study found that KGM/CMCS composite films can be used to cross-link epigallocatechin-gallate for the preparation of biocomposite films,[7] which provides valuable insights into the improvement of KGM and CMCS applications, but it is regrettable that there remains a lack of comprehensive research on KGM/CMCS composite films at present.

With the increasing demand for naturally bioavailable packaging materials, there is a growing focus on developing bio-based films that exhibit enhanced bioactivity to fulfill a wider range of practical needs. The addition of active substances (essential oils, polyphenols, *etc.*) or other functional ingredients is an effective

[a]*Fujian Vocational College of Bioengineering, No. 42, Hongshan Bridge Zhongdian, Cangshan District, Fuzhou 350007, China*

[b]*College of Food Science, Fujian Agriculture and Forestry University, Fuzhou, Fujian 350002, China. E-mail: pang3721941@163.com; chwu0283@163.com*

† These authors contributed equally to the manuscript.

way to improve the quality and performance of film.[8,9] ZnO nanoparticles (ZNPs) are a commonly used functional metal oxide nanoparticles with favorable antimicrobial and photocatalytic properties, which are widely utilized in food and medicine industries. Li *et al.* successfully utilized a combination of ZNPs and chitosan to create films with exceptional antimicrobial properties for preserving cherry tomatoes.[10] Similarly, Zheng *et al.* discovered that ZNPs can improve the mechanical properties and antimicrobial activity of chitosan-coixen starch membrane films.[11] Additionally, to further enhance the performance of bio-based films, active substances with different properties can be synergistically incorporated into polymer films. The combination of ZNPs and essential oils (EOs) has been proven effective in enhancing the properties of polymer films.[12]

Oregano essential oil (OEO) is extracted from natural oregano leaves and possesses remarkable antibacterial and antioxidant properties.[13] However, it is often unsatisfactory simply add EOs to the films. EOs are not adequately stabilized and are susceptible to environmental factors such as light, oxygen, and temperature,[14] and are prone to phase separation from the film substrate during the film formation process.[15] Encapsulation of EOs using Pickering emulsion is an effective strategy to improve the stability and bioactivity of EOs.[16] Additionally, the incorporation of OEO into polymer films in the form of Pickering emulsions offers improved film properties.[17] OEO and ZNPs are promising for the development of bio-based films. However, according to our knowledge, there are no studies on the synergistic improvement of the properties of KGM/CMCS films by OEO Pickering emulsion and ZNPs.

The goal of current work was the preparation and characterization of innovative KGM/CMCS nanocomposite film containing OEO Pickering emulsion and ZNPs. The effect of OEO Pickering emulsion, ZNPs and their combinations on the physical–mechanical properties (optical properties, water vapor barrier and thermal stability, *etc.*) and microstructure of KGM/CMCS nanocomposite films. Moreover, the antimicrobial activity of the nanocomposite films was also discussed by inhibition circle experiments. We hope this work will serve as valuable reference for the development of new natural biopreservation films.

2. Materials and methods

2.1 Materials

KGM (purity > 90%) was purchased from San Ai Konjac Food Co. Ltd (Sichuan, China). OEO and CMCS (carboxylation ≥80%) were supplied by Yuan Ye Biotechnology Co. Ltd (Shanghai, China). ZNPs (purity 99%) were purchased from McLean Biochemistry & Technology Co. Carboxylated-cellulose nanocrystals (C-CNCs, carboxylation content 1.9 mmol g^{-1}) were provided by Guilin Qihong Technology Co Ltd (Guangxi, China). All other chemical reagents were of analytical grade.

2.2 Preparation of OEO Pickering emulsion

The C-CNCs were added to 95 mL of water at a concentration of 2% (w/v), magnetically stirred for 30 min and then homogenized at 10 000 rpm for 20 min to obtain the C-CNCs suspension. Then 2 mL of OEO and 3 mL of soybean oil were added to the above suspension together and homogenized at 13 000 rpm for 4 min to prepare the OEO Pickering emulsion.

2.3 Preparation of nanocomposite films

Nanocomposite films were prepared by reference to the previous method with slight modifications.[18] Precisely, KGM powder was added to deionized water at a concentration of 1% (w/v) and stirred magnetically for 4 h at 60 °C for full dissolution. CMCS powder was dispersed in deionized water at 1% (w/v) concentration overnight with stirring. The KGM and CMCS solutions obtained above were mixed in the ratio of 7 : 3 and stirred for 30 min to obtain KGM/CMCS mixture. Additionally, ZNPs and OEO Pickering emulsion were added to the KGM/CMCS mixed solution separately or mixed such that the concentrations of ZNPs and OEO Pickering emulsion were 0.15% (w/v) and 30% (v/v) of the overall solution, respectively. The different film samples were recorded as KC, KCZ, KCP, KCZP. Furthermore, to obtain nanocomposite films with less brittleness and easy handling, glycerol at 0.2% (v/v) of the total volume of the mixture was added as a plasticizer. In a plastic culture dish with a thickness of 9 cm, pour 30 mL of the mentioned mixture and allow it to dry at 45 °C for 24 h. Subsequently, carefully remove the dried nanocomposite film from the surface of the dish. To ensure consistent conditions, place the film samples in a temperature and humidity chamber at a constant temperature of 25 °C and a relative humidity of 50% for a minimum period of 72 h.

2.4 Characterization of OEO Pickering emulsion

2.4.1 Droplets size. The droplet size of OEO Pickering emulsion was measured by laser particle size analyzer (Malvern Instruments Ltd, UK) and the mean diameter ($D[4,3]$) was selected to represent the droplet size. The refractive indices of the dispersed and continuous phases were 1.4991 and 1.333, respectively. The emulsion was diluted 1000 times with deionized water to avoid multiple scattering and stirred at 2000 rpm.

2.4.2 Microscopic morphology. The morphology of OEO Pickering emulsion droplets was observed through an optical microscope (Zeiss, Germany). Take a small drop of sample and add it to a glass slide before observation and cover with a coverslip.

2.5 Rheological properties of composite solutions

The apparent viscosity and viscoelastic properties of the composite solutions were evaluated by an oscillatory rheometer (MCR 301, Anton Paar, St. Laurent, QC, Canada) equipped with a 50 mm plate. The tests were performed at 25 °C, the viscosity was recorded in the shear rate range of 0.1–1000 s^{-1}, and the storage (G') and loss (G'') modulus were measured in the scanning range of 1–100 rad s^{-1} at a strain of 1%.

2.6 Characterization of nanocomposite films

2.6.1 Fourier transform infrared (FT-IR) spectroscopy. The chemical structure of the nanocomposite films was analyzed by using a FT-IR spectrometer (Thermo Nicolette 6700, Thermo Nicolet, USA) with reference and slight modification to Yu *et al.*[19] The samples were mixed with KBr powder in the ratio of 1 : 100 and pressed into thin sheets, then scanned in the wave number range of 4000–400 cm^{-1} and the spectra were recorded.

2.6.2 X-ray diffraction (XRD). XRD patterns were scanned using an X-ray diffractometer (Bruker, Germany) for the nanocomposite films. All samples were scanned at 25 °C at a rate of 2° min^{-1} over a range of 5–70° at 40 kV.

2.6.3 Microstructure. The morphology of the nanocomposite films was observed using scanning electron microscopy (SEM) (SU 8010, Hitach, Japan) according to previously reported method.[20] The films were fixed on aluminium stubs and covered with gold spray under vacuum before testing.

2.6.4 Color. The colorimetric parameters of nanocomposite films were measured using a colorimeter (Beijing Chentek Instrument Technology Co., Ltd, China). A white standard color plate ($L^* = 96.031$, $a^* = 0.28$, $b^* = -0.724$) was used for calibration prior to testing, and the L^*, a^*, and b^* parameters in the CIELAB space were recorded to evaluate the apparent color of the films. The total colour difference (ΔE) follows the previous method calculated with eqn (1).[21]

$$\Delta E = \sqrt{(\Delta L^*)^2 + (\Delta a^*)^2 + (\Delta b^*)^2} \quad (1)$$

where ΔL^*, Δa^*, Δb^* are the L^*, a^*, b^* differences between the film sample and the white standard color plate, respectively.

2.6.5 Light transmittance. The transmittance of the nanocomposite films was tested using UV-vis spectrometer (UV300, InsMark, China). The films were cut into 1 × 4 cm^2 into the spectrometer and the absorption spectrum in the range of 500–600 nm was recorded.

2.6.6 Water vapor permeability (WVP). The WVP of the films was determined based on the previously defined method with some modifications.[22] 3 g of dried $CaCl_2$ was taken in a weighing bottle and sealed with a film samples. The weighing bottle was placed in a desiccator at 25 °C and 60% relative humidity. The weight of the bottle was recorded every 24 h. The WVP calculated according to eqn (2).

$$\mathrm{WVP}(\text{g mm per m}^2 \text{ per day per kPa}) = \frac{\Delta W/\Delta t \times S}{\Delta P} \times T \quad (2)$$

where Δw is the weight added to the weighing bottle (g), Δt is the time of placement (days), S is the exposed surface area of the film (m^2), T is the thinness of the film (mm), ΔP is the differential pressure of water vapor on the film (Pa) ($\Delta P = 3.282$ kPa at 25 °C).

2.6.7 Thermal stability. The thermogravimetric analysis (TGA) of the films was carried out using a simultaneous thermogravimetric analyzer (DSC-214, Netzsch, Germany) to assess the thermal stability of the films. ~8 mg of the film samples was placed in a vessel and heated from 30 °C to 600 °C at a rate of 10 °C min^{-1} under a stream of nitrogen.

2.6.8 Antibacterial activity. The antibacterial activity was measured by the disc diffusion method for nanocomposite films, which was referred to the previously reported method with slight modifications.[23] *E. coli* and *S. aureus* were selected as test bacteria. The bacterial stock suspension was first inoculated onto LB broth medium and incubated at 37 °C for 12 h with shaking at 120 rpm to maintain the cells in stationary growth phase. 80 μL of the cultured bacterial suspension was spread on LB agar plates. Then, a film with a diameter of ~9 mm was placed on the agar surface. The plates were then incubated at 37 °C for 24 h. The antibacterial activity was reflected by the size of the inhibition circle.

2.7 Statistical analysis

All the tests were conducted in triplicate and the experimental data were expressed as means ± standard deviation (SD). Analysis of variance (ANOVA) and significance tests were performed using SPSS software. $p < 0.05$ was regarded as statistically significant.

3. Result and discussion

3.1 Characterization of OEO Pickering emulsion

The stability and droplet size of Pickering emulsion play a significant role in influencing the structural and mechanical properties of nanocomposite films.[24] Fig. 1a and b show the droplet size distribution and micro morphology of OEO Pickering emulsion. The average droplet diameter of OEO Pickering emulsion was 48.43 ± 3.56 μm, with a well-concentrated droplet size distribution. It is observed from the microscopic images that the droplets of OEO Pickering emulsion are spherical, exhibiting a relatively uniform size, and can be stably dispersed in water. To further explore the stability of the emulsions, we recorded photographs of the emulsion from before and after 14 days of standing (Fig. 1c), and the OEO Pickering emulsion remained uniform and stable with no breakage of the emulsion. This demonstrates the excellent stability of Pickering emulsion stabilized with C-CNCs.

3.2 Rheological properties of composite solutions

Rheological properties affect the structure, spread-ability and mechanical properties of biopolymer solutions directly. Fig. 2a shows the viscosity of the nanocomposite solutions as a function of shear rate. The viscosity of all the samples shows a decreasing trend with the shear rate increased, showing a shear thinning behavior, which is a common characteristic of pseudoplastic fluids.[25] It is evident that the addition of ZNPs and Pickering emulsion can improve the viscosity of the composite solution, particularly when both are added simultaneously. The incorporation of ZNPs into the entangled network structure of KGM and CMCS effectively eliminates free volume within the matrix, resulting in an increase in viscosity, which is in agreement with previous finding.[26] Previous research has reported that the addition of essential oils leads to a decrease in viscosity.[27] but we found that the addition of OEO Pickering emulsion improved the viscosity significantly, which may be

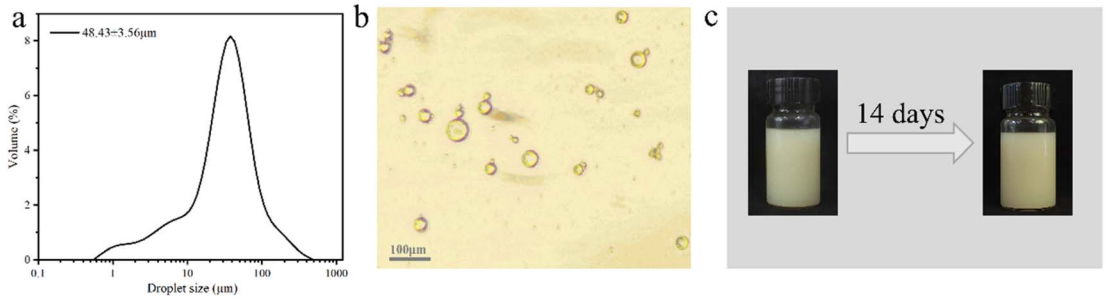

Fig. 1 Droplet distribution (a) and micrograph (b) of OEO Pickering emulsion, photograph of the appearance of OEO Pickering emulsion before and after 14 days of placement (c).

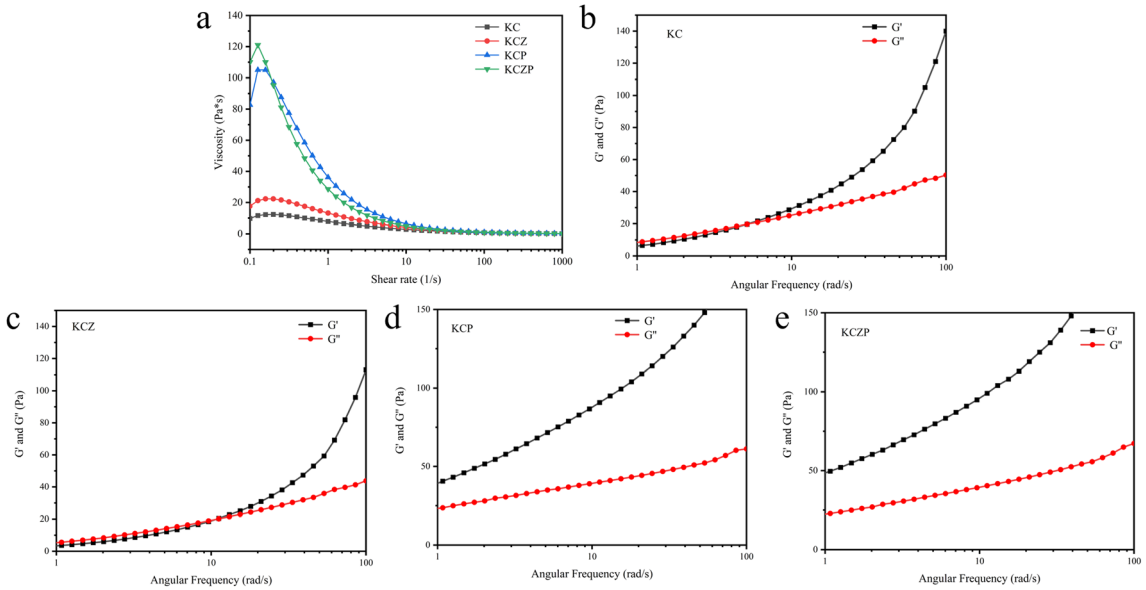

Fig. 2 Rheological behavior of nanocomposite solutions, viscosity as a function of shear rate (a) and G′ and G″ as a function of angular frequency (b–e).

attributed to the effect of emulsifiers C-CNCs. C-CNCs have strong interactions with KGMs including hydrogen bonding and chain entanglement, and this plays a positive role in enhancing the viscosity of the system.[28]

The dynamic rheological properties serve as indicators of interaction and structural characteristics within the composite solution. Fig. 2b–e depicts the relationship between the loss modulus (G') and storage modulus (G'') of nanocomposite solutions as a function of angular frequency. The G' and G'' tend to increase gradually with increasing angular frequency for all the samples in the range of 1–100 rad s^{-1}. It should be noted that for both KC and KCZ samples showcase an intersection at higher angular frequencies, indicating that the composite solution changes from a liquid-like to elastic-solid behavior with increasing angular frequency. This is explained by the fact that the molecular chains of the composite solution are easily relaxed and untangled during long period oscillations at low angular frequencies, thus the system behaves as a viscous fluid. Whereas at high angular frequency the oscillations are short and the molecular chains can resist disentanglement and allow the formation of a temporary three-dimensional network structure, resulting in elastic-solid like state of the system.[29] The dynamic rheological properties of the composite solution underwent significant changes after doping with OEO Pickering emulsion, where G' consistently surpassing G'', displaying a more pronounced solid behavior. The cross-linking of the C-CNCs with the KGM contributes to the improvement of the mechanical strength of the solution.[28] In addition, the potential hydrogen bonding interactions between ZNPs and the polymer have the potential to enhance the network structure and, consequently, improve the rheological properties.[30]

3.3 Characterization of nanocomposite films

3.3.1 FT-IR. The interactions between the components in the film were probed by FT-IR. As shown in Fig. 3, the main peaks of KC are at 3442, 2924, 1631, and 1417 cm^{-1}, which correspond to the –OH stretching, the –CH vibration, and the

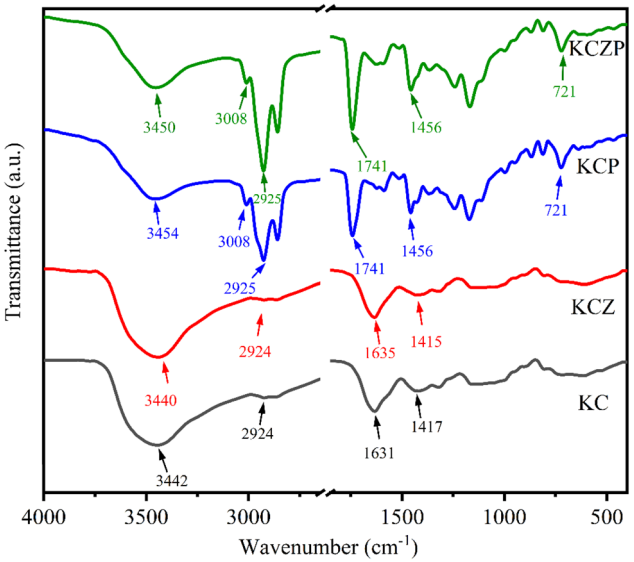

Fig. 3 FT-IR spectra of nanocomposite films.

symmetric and asymmetric stretching vibrations of COO–, respectively.[7,31] The peak at 3442 cm^{-1} is shifted towards lower wave numbers upon addition of ZnO, which is attributed to the hydrogen bonding interaction between ZnO and KC.[32] The infrared spectra of the films were significantly altered after incorporation of Pickering emulsion, which is related to the inclusion of OEO and C-CNCs. The drastic shift in the O–H absorption peak at 3442 cm^{-1} suggests hydrogen bonding interactions between KC and C-CNCs.[28] Additionally, interactions between OEO and free hydroxyl groups contribute to the shift in O–H absorption peak.[17] Notably, the typical characteristic peaks of KC are present in all film samples, indicating that the addition of ZNPs and emulsions to the KC matrix does not affect the chemical structure of the KC film, merely involving non-covalent bonding interactions.

3.3.2 XRD. The XRD patterns provide valuable insights into the compatibility and crystal structure of the films. As shown in Fig. 4, the characteristic peaks of all samples display broader diffraction patterns, indicating their amorphous nature. The characteristic peaks of ZNPs (PDF # 99-0111) are not obvious in the films, suggesting that the ZNPs are well encapsulated in the films in an amorphous state. The addition of appropriate amount of ZNPs does not significantly change the crystal structure of KC, which is consistent with the results of previous study.[26] The original peak at 22° enhanced and slightly shifted to the left after mixing with OEO Pickering emulsion, and a new peak appeared at 13°. The two diffraction peaks at 14.6° (101) and 22.7° (200) are found to be related to the crystal structure of C-CNCs in a previous study,[33] thus it can be reasonably deduced that the change in the pattern is due to the crystal structure of C-CNCs. Furthermore, the enhancement and shift of the peaks suggest an interaction between the OEO Pickering emulsion and KC, corroborating the findings from FT-IR analysis.

3.3.3 Microstructure. The microscopic morphology of the films was observed by SEM (Fig. 5). The surface of the KC films is relatively smooth, and the internal structure is dense and without pores. The apparent circular bumps appear on the surface of the film after incorporating ZNPs, yet there are no visible pores, demonstrating that the ZNPs are well encapsulated inside the film. However, the surface and cross-section of the film became uneven after the addition of OEO Pickering emulsion, while obvious pores appeared in the cross-section, which was caused by the embedding of OEO in the film matrix through the emulsion. Similar phenomena have been observed in previous report by Xu *et al.*[17] Furthermore, the instability of the emulsion during the drying process contributed to the irregularity on the surface of films.[34]

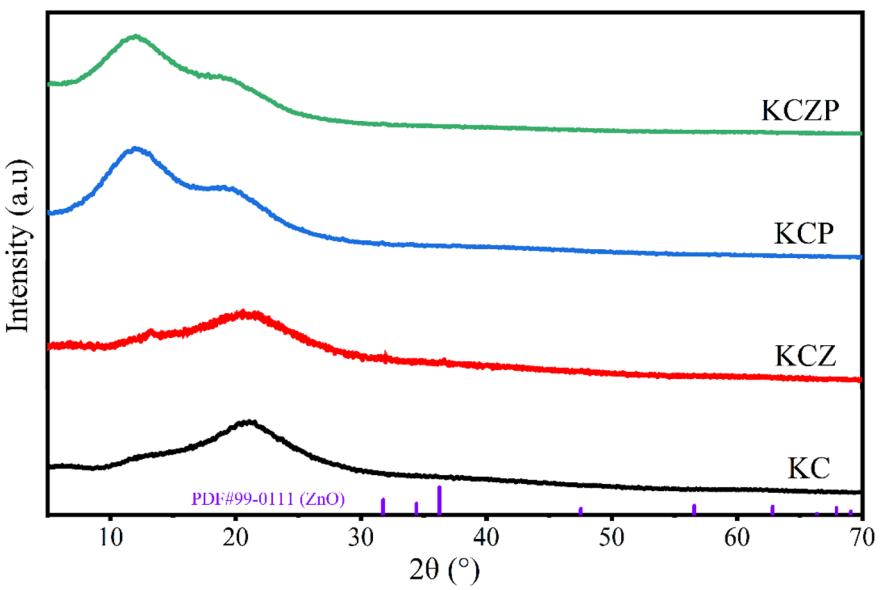

Fig. 4 XRD patterns of nanocomposite films.

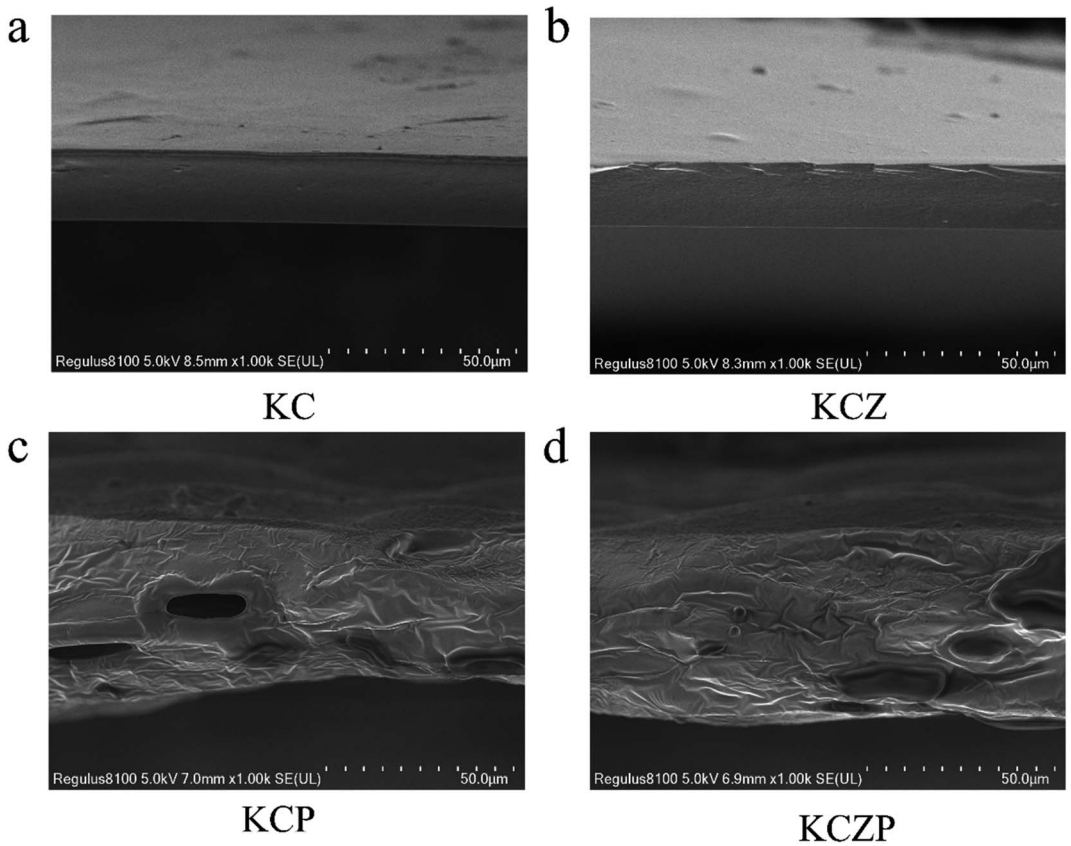

Fig. 5 SEM images of nanocomposite films.

Table 1 Color parameters of nanocomposite films

Example	L^*	a^*	b^*	ΔE^*
KC	89.88 ± 0.41^a	1.44 ± 0.12^b	-6.04 ± 0.64^d	8.22 ± 0.71^c
KCZ	87.10 ± 0.67^b	1.59 ± 0.03^a	-2.46 ± 0.28^c	9.19 ± 0.92^c
KCP	81.96 ± 1.30^c	0.25 ± 0.05^d	0.42 ± 0.07^b	14.12 ± 1.29^b
KCPZ	80.52 ± 0.66^c	1.09 ± 0.04^c	4.68 ± 0.55^a	16.45 ± 0.76^a

Data not sharing the same superscript letter in the same parameter are significantly different ($P < 0.05$).

3.3.4 Color. The color parameters of the films are shown in Table 1. The KC film has the highest brightness (highest L^* value) as compared to the film containing ZNPs and OEO Pickering emulsion. The a^* and b^* values of the films increased with the addition of ZNPs, which represents a more pronounced green and yellow coloration of the films. It is consistent with the previously reported finding that ZNPs can increase the a^* and b^* values of chitosan-carboxymethyl cellulose films.[35] The incorporation of OEO Pickering emulsion leads to a further intensification of the yellow coloration of the film, owing to the accumulation of yellowish oregano essential oil inside the film, which interferes with light transmission, or due to the presence of droplets of the emulsion enhancing the scattering effect.[36] ΔE^* used to indicate the color difference between the color of the film and standard white. Increase in ΔE of a nanocomposite film demonstrates an intensity of the color of the film, which contributes to the protection of packaged food from visible and ultraviolet light.[37]

3.3.5 Light transmittance. Light is an important factor in food spoilage and leads to rapid oxidation of lipids in food, therefore it is necessary to evaluate the light barrier properties of films. Fig. 6 displays the transmittance (T%) of the films in

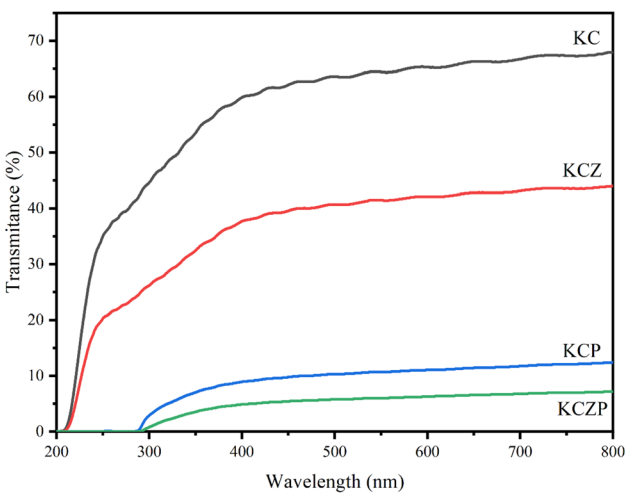

Fig. 6 Light transmission of nanocomposite films.

the wavelength range of 200–800 nm. Low transmittance means that the film is effective in shielding against UV light, and KC films have the highest transmittance, which is related to their highly transparent and colorless nature. ZNPs and Pickering emulsions have a positive effect on reducing the transmittance of the films. The high refractive index, wide band gap and excitation binding ability of ZNPs are favorable for blocking the passage of UV rays.[38] The distribution of OEO Pickering emulsion oil droplets inside the film blocks the light passage. In addition, the light scattering effect of the oil droplets results in the blockage of UV light transmission.[39] The excellent UV blocking ability of KCZP films benefits from the synergistic effect of the ZNPs and the Pickering emulsion.

3.3.6 WVP. It is well known that moisture has a significant effect on food spoilage, and the water vapor barrier properties of films often reveal their suitability for food packaging. A lower value of water vapor permeability (WVP) corresponds to a higher ability of the film to resist water transfer. KC films have the highest WVP (Fig. 7), which may be due to the hydrophilic nature of KGM.[2] The water barrier properties of the film can be enhanced by both OEO Pickering emulsion and ZNPs. The introduction of Pickering emulsion droplets into the KC matrix extends the tortuous path for water molecules to traverse through the film.[40] The intermolecular interactions between KGM, CMCS and ZNPs resulted in a denser structure of the films.[26] An interesting point is that KCP film outperform KCZ and KCZP films in terms of water vapor barrier properties, which may be related to the pore structure observed in the SEM (Fig. 5). The distribution of emulsion droplets within the KC matrix disrupts its original dense structure, leading to the formation of irregular pores and internal cavities, which facilitate the diffusion of water vapor. Similar observation was reported previously that essential oil Pickering emulsions reduce the water barrier capacity of polysaccharide-based films.[41]

3.3.7 Thermal stability. The thermal stability of the films was assessed through thermogravimetric analysis (TGA), as shown in Fig. 8). The mass loss of the film occurred in three stages. The stage I (30–230 °C) is attributed to the evaporation of free and loosely bound water in the film, the stage II (230–480 °C) corresponds to the thermal decomposition of the polymer molecular chains and the release of the essential oils, and the stage III is the carbonization of the material.[42] KCZ exhibits fewer mass losses in the II and III stages compared to KC, suggesting that the addition of ZNPs enhances the thermal stability of the films, which may be attributed to the interaction between ZNPs and KC facilitating the formation of a more compact network structure within the films.[9] The TG curves changed significantly in the stage I and II mass loss with the addition of OEO Pickering emulsion. This can be attributed to the lower moisture content present in the KCP and KCZP film systems compared to KC and KCZ films, as well as the presence of OEO. The reduced moisture content led to less mass loss from water evaporation during the first stage of KCP and KCPZ films, and the degradation of the essential oil at high temperatures mainly affects the mass loss in the second stage. Also, the KCPZ films show better thermal stability than KCP owing to the addition of ZNPs.

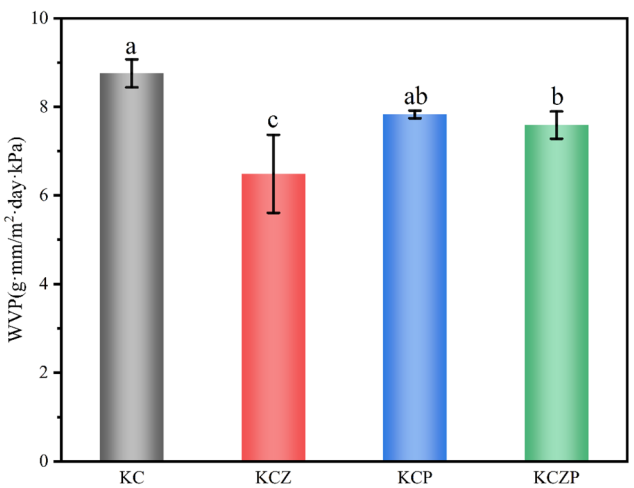

Fig. 7 WVP of nanocomposite films.

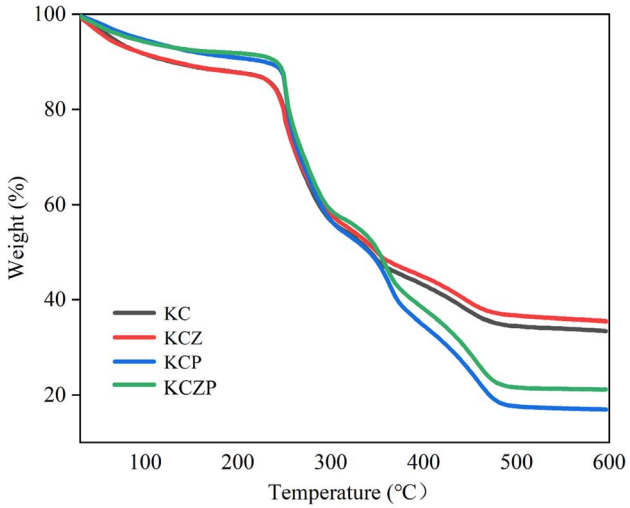

Fig. 8 TGA curves of nanocomposite films.

3.3.8 Antibacterial activity. Gram-negative (*E. coli*) and positive (*S. aureus*) bacteria were selected as experimental microorganisms to evaluate the antimicrobial activity of the films. The results are shown in Fig. 9), pure KC film has no antibacterial activity against both *E. coli* and *S. aureus*, and the doping of ZNPs and OEO Pickering emulsion appear different trends in the inhibition of *E. coli* and *S. aureus* by the films. It is clear that the ZNPs and OEO Pickering emulsion enabled the films to inhibit *S. aureus* better than *E. coli*, in particular the KCZP film performed extremely strong inhibition of *S. aureus*. ZNPs and OEO are common bacteriostatic agents. ZNPs damage cell membranes by adsorbing onto bacterial surfaces, while releasing Zn^{2+} ions which are toxic to bacterial growth and metabolism.[43] Phenolic ring compounds such as terpenoids (*e.g.* thymol, carvacrol) and phenolic acids (*e.g.* rosmarinic acid) contained in OEO disrupt the structure of bacterial cell membranes, interrupt bacterial metabolic pathways and thus inhibit bacterial reproduction.[44] The difference in the

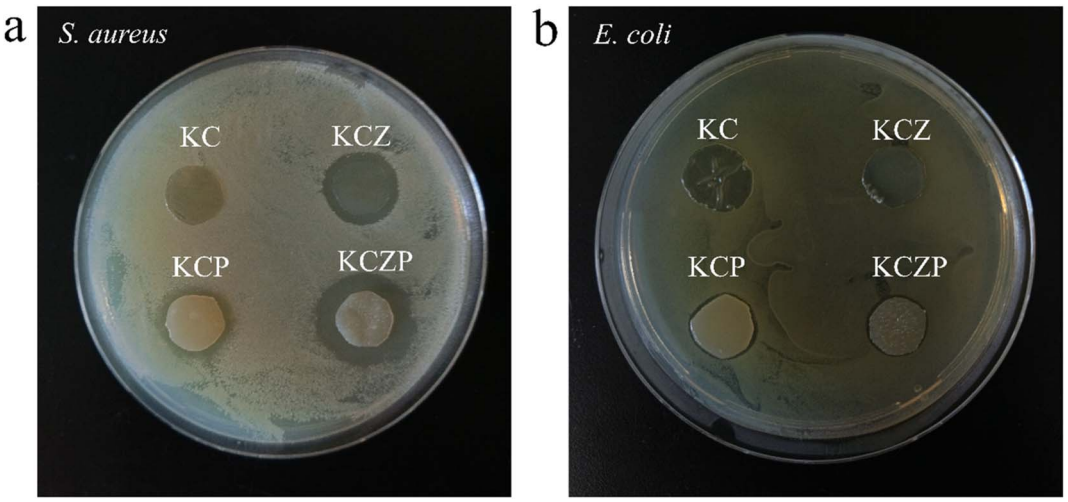

Fig. 9 Photographs of inhibition zones of nanocomposite films against *S. aureus* (a) and *E. coli* (b).

antibacterial effect of the films on *E. coli* and *S. aureus* may be due to the difference in their cell wall structures; *E. coli* is a Gram-negative bacterium, and the outer membrane around its cell wall restricts the diffusion of hydrophobic actives through its lipopolysaccharide cover layer.[45]

4. Conclusion

In this study, KGM/CMCS nanocomposite films containing OEO Pickering emulsion and ZNPs were successfully prepared, and evaluated the effects of OEO Pickering emulsion and ZNPs on the physical and structural properties and antimicrobial activities of the films. The particle size of OEO Pickering emulsion was 48.43 ± 3.56 μm, and it had well dispersion and stability. The OEO Pickering emulsion and ZNPs increased the viscosity and viscoelastic modulus of the KGM/CMCS composite solution, which was mainly due to the hydrogen bonding interactions between the Pickering emulsion, ZNPs and KC matrix as revealed by the FT-IR and XRD results. The SEM observed that the Pickering emulsion and ZNPs were well incorporated into the KC matrix and formed fine pores on the films. The OEO Pickering emulsion and ZNPs result in an increase in the color intensity of the film and an increase in the UV and water vapor barrier. TGA results demonstrate that ZNPs are favorable for enhancing the thermal stability of the film, but the thermal decomposition of the essential oils in the Pickering emulsions leads to an increase in the heat loss. Antimicrobial experiments showed that the incorporation of OEO Pickering emulsion and ZNPs improved the antimicrobial properties of the films, especially the best inhibition of *S. aureus* when both were added simultaneously. This study verifies the feasibility of the developed films for food preservation packaging applications and provides reference to valuable implications for the development of natural bio-composite films.

Author contributions

Zhibin Pan: conceptualization, data curation, writing – original draft, visualization. Weiquan Zhong: methodology, formal analysis, investigation. Jingting Xu: formal analysis, investigation, writing – review & editing. Danjie Li: data curation, writing – review & editing. Junhan Lin: resources, writing – review & editing. Weibin Wu: writing – review & editing, project administration. Jie Pang: writing – review & editing, project administration, funding acquisition. Chunhua Wu: writing – review & editing, funding acquisition.

Conflicts of interest

The authors declare that they have no conflict of interest in the publication of this article.

Acknowledgements

This work was supported by the National Natural Science Foundation of China (Grant No. 31801616).

References

1 U. Amin, M. U. Khan, Y. Majeed, M. Rebezov, M. Khayrullin, E. Bobkova, M. A. Shariati, I. M. Chung and M. Thiruvengadam, *Int. J. Biol. Macromol.*, 2021, **183**, 2184–2198.
2 Y. Ni, Y. Liu, W. Zhang, S. Shi, W. Zhu, R. Wang, L. Zhang, L. Chen, J. Sun, J. Pang and J. Wang, *LWT*, 2021, **152**, 112338.
3 A. L. Bukzem, R. Signini, D. M. dos Santos, L. M. Lião and D. P. R. Ascheri, *Int. J. Biol. Macromol.*, 2016, **85**, 615–624.
4 R. Bai, X. Zhang, H. Yong, X. Wang, Y. Liu and J. Liu, *Int. J. Biol. Macromol.*, 2019, **126**, 1074–1084.
5 P. Zimet, Á. W. Mombrú, D. Mombrú, A. Castro, J. P. Villanueva, H. Pardo and C. Rufo, *Carbohydr. Polym.*, 2019, **219**, 334–343.
6 W. Xie, Y. Du, S. Yuan and J. Pang, *Int. J. Biol. Macromol.*, 2021, **180**, 385–391.
7 J. Sun, H. Jiang, M. Li, Y. Lu, Y. Du, C. Tong, J. Pang and C. Wu, *Food Hydrocolloids*, 2020, **105**, 105756.

8 S. Zhang, Z. He, F. Xu, Y. Cheng, G. I. N. Waterhouse, D. Sun-Waterhouse and P. Wu, *Food Hydrocolloids*, 2022, **124**, 107222.
9 J. Liu, Y. Wang, Y. Liu, S. Shao, X. Zheng and K. Tang, *Int. J. Biol. Macromol.*, 2023, **239**, 124361.
10 Y. Li, Y. Zhou, Z. Wang, R. Cai, T. Yue and L. Cui, *Foods*, 2021, **10**(12), 3135.
11 K. Zheng, J. Zhang, F. Yang, W. Wang, W. Li and C. Qin, *Lwt*, 2022, **164**, 113665.
12 T. Gasti, S. Dixit, V. D. Hiremani, R. B. Chougale, S. P. Masti, S. K. Vootla and B. S. Mudigoudra, *Carbohydr. Polym.*, 2022, **277**, 118866.
13 W. Zduńczyk, K. Tkacz and M. Modzelewska-Kapituła, *Foods*, 2023, **12**(10), 2013.
14 M. Wu, J. Yang, S. Chen, P. Lu and R. Wang, *Carbohydr. Polym.*, 2021, **274**, 118654.
15 H. Almasi, S. Azizi and S. Amjadi, *Food Hydrocolloids*, 2020, **99**, 105338.
16 J. Hu, H. Zhu, Y. Feng, M. Yu, Y. Xu, Y. Zhao, B. Zheng, J. Lin, W. Miao, R. Zhou and P. J. Cullen, *Food Chem.*, 2023, **421**, 136201.
17 J. Xu, M. He, C. Wei, M. Duan, S. Yu, D. Li, W. Zhong, C. Tong, J. Pang and C. Wu, *Food Hydrocolloids*, 2023, **139**, 108539.
18 J. Sun, Y. Du, J. Ma, Y. Li, L. Wang, Y. Lu, J. Zou, J. Pang and C. Wu, *Int. J. Biol. Macromol.*, 2019, **138**, 866–873.
19 S. Yu, M. Duan, R. Zeng, F. Chen, W. Zhong, J. Sun, J. Xu, D. Li, Y. Zheng, X. Liu, J. Pang and C. Wu, *Int. J. Biol. Macromol.*, 2023, **233**, 123492.
20 S. B. H. Hashim, H. E. Tahir, A. A. Mahdi, J. Zhang, X. Zhai, Q. A. Al-Maqtari, C. Zhou, G. K. Mahunu, Z. Xiaobo and S. Jiyong, *Food Chem.*, 2024, **432**, 137203.
21 T. M. Vieira, M. Moldão-Martins and V. D. Alves, *Foods*, 2021, **10**(7), 1654.
22 R. A. Ilyas, S. M. Sapuan, M. R. Ishak and E. S. Zainudin, *Carbohydr. Polym.*, 2018, **202**, 186–202.
23 W. Zhong, Z. Zhi, J. Zhao, D. Li, S. Yu, M. Duan, J. Xu, C. Tong, J. Pang and C. Wu, *J. Agric. Food Chem.*, 2022, **70**(42), 13778–13786.
24 M. Wu, Z. Zhou, J. Yang, M. Zhang, F. Cai and P. Lu, *Int. J. Biol. Macromol.*, 2021, **190**, 433–440.
25 C. Wu, Y. Li, J. Sun, Y. Lu, C. Tong, L. Wang, Z. Yan and J. Pang, *Food Hydrocolloids*, 2020, **98**, 105245.
26 J. Sun, H. Jiang, H. Wu, C. Tong, J. Pang and C. Wu, *Food Hydrocolloids*, 2020, **107**, 105942.
27 Z. Liu, D. Lin, N. Li and X. Yang, *Food Hydrocolloids*, 2022, **124**, 107330.
28 C. Tong, S. Jiang, D. Ye, K. Li, J. Liu, X. Zeng, C. Wu and J. Pang, *Food Hydrocolloids*, 2023, **142**, 108812.
29 X. Luo, P. He and X. Lin, *Food Hydrocolloids*, 2013, **30**, 92–99.
30 R. Santhosh and P. Sarkar, *Food Hydrocolloids*, 2022, **133**, 107917.
31 F. Wahid, J.-J. Yin, D.-D. Xue, H. Xue, Y.-S. Lu, C. Zhong and L.-Q. Chu, *Int. J. Biol. Macromol.*, 2016, **88**, 273–279.
32 H. Zhang, Y. Fu, F. Niu, Z. Li, C. Ba, B. Jin, G. Chen and X. Li, *Food Hydrocolloids*, 2018, **81**, 104–112.
33 S. Hu, Z. Qin, M. Cheng, Y. Chen, J. Liu and Y. Zhang, *Cellulose*, 2018, **25**, 1883–1898.
34 M. Xiao, L. Luo, B. Tang, J. Qin, K. Wu and F. Jiang, *LWT*, 2022, **154**, 112683.
35 N. Noshirvani, B. Ghanbarzadeh, R. R. Mokarram, M. Hashemi and V. Coma, *Int. J. Biol. Macromol.*, 2017, **99**, 530–538.
36 Q.-R. Liu, W. Wang, J. Qi, Q. Huang and J. Xiao, *Food Hydrocolloids*, 2019, **87**, 165–172.
37 V. A. Pereira, I. N. Q. de Arruda and R. Stefani, *Food Hydrocolloids*, 2015, **43**, 180–188.
38 W. Zhang, M. A. Sani, Z. Zhang, D. J. McClements and S. M. Jafari, *Int. J. Biol. Macromol.*, 2023, **230**, 123188.
39 P. Tongnuanchan, S. Benjakul and T. Prodpran, *Food Chem.*, 2012, **134**, 1571–1579.
40 L. E. Velásquez-Castillo, M. A. Leite, V. J. A. Tisnado, C. Ditchfield, P. J. d. A. Sobral and I. C. F. Moraes, *Foods*, 2023, **12**(3), 576.
41 S. Roy and J.-W. Rhim, *Colloids Surf., A*, 2021, **627**, 127220.
42 M. Ji, J. Li, F. Li, X. Wang, J. Man, J. Li, C. Zhang and S. Peng, *Carbohydr. Polym.*, 2022, **281**, 119078.
43 S. M. Eskandarabadi, M. Mahmoudian, K. R. Farah, A. Abdali, E. Nozad and M. Enayati, *Food Packag. Shelf Life*, 2019, **22**, 100389.
44 Y. Zhou, S. Sun, W. Bei, M. R. Zahi, Q. Yuan and H. Liang, *Int. J. Biol. Macromol.*, 2018, **112**, 7–13.
45 S. Burt, *Int. J. Food Microbiol.*, 2004, **94**, 223–253.